Glucose-driven TRIB3 enhances the tumorigenic potential of colon cancer via the PI3K/AKT pathway

YUNTING BAI[1*], XUYING HUANG[1,2*], GUANGYU AN[1], YANG GE[1], RUI YAN[1] and DAN YU[1]

[1]Department of Oncology, Beijing Chao Yang Hospital, Capital Medical University, Beijing 100020, P.R. China;
[2]China Institute for Cancer, Chinese Institutes for Medical Research, Beijing 100069, P.R. China

Received August 6, 2025; Accepted February 10, 2026

DOI: 10.3892/mmr.2026.13842

Abstract. Diabetes, characterized by chronic hyperglycemia, is closely associated with worse outcomes in patients with colorectal cancer (CRC). However, the mechanism underlying the influence of high glucose levels on CRC prognosis has not yet been fully elucidated. Tribbles 3 (TRIB3) protein, a unique pseudokinase, has been implicated as an intermediary between metabolism and oncogenesis. The present study aimed to elucidate whether TRIB3 is modulated by elevated glucose levels in CRC and contributes to the malignant behavior of diabetic CRC tumors. TRIB3 expression was detected using immunohistochemistry in colon cancer tissues from patients with and without diabetes. Following the knockdown of TRIB3 by short hairpin RNA, colon cancer cell proliferation and migration were assessed using Cell Counting Kit-8 and Transwell assays. Additionally, changes in the expression of related genes were detected using reverse transcription-quantitative PCR, western blotting and immunofluorescence staining. The present study detected significant upregulation of TRIB3 in diabetic CRC. In addition, the findings indicated that TRIB3 may promote epithelial-mesenchymal transition (EMT) by activating the PI3K/AKT signaling pathway, thereby enhancing the malignant characteristics of CRC. By contrast, TRIB3 knockdown in CRC cells mitigated glucose-induced proliferation, invasiveness and EMT progression. In conclusion, TRIB3 may be modulated by increased glucose levels, subsequently contributing to the malignancy of tumor cells in diabetic CRC by modifying EMT status. These findings underscore the potential of TRIB3 as a therapeutic target for effective management of patients with diabetic and CRC.

Correspondence to: Dr Dan Yu or Dr Rui Yan, Department of Oncology, Beijing Chao Yang Hospital, Capital Medical University, 8 South Gongti Road, Beijing 100020, P.R. China
E-mail: xiaoyugw@126.com
E-mail: yrui2019@126.com

*Contributed equally

Key words: colon cancer, high glucose, tribbles 3, epithelial-mesenchymal transition, PI3K/AKT pathway

Introduction

Cancer poses a global health threat, and 8-18% of individuals with cancer have diabetes as a concurrent health issue (1,2). Hyperglycemia, characterized by abnormally high blood glucose levels, is a crucial diagnostic marker for diabetes, and serves a notable role in both the initiation and progression of cancer (3). Numerous epidemiological investigations have revealed that individuals with diabetes are at a heightened risk of various types of cancer, including liver, pancreatic, stomach, kidney, breast and colorectal cancer (CRC) (4,5).

Several studies have revealed that hyperglycemia, particularly that associated with type II diabetes mellitus, is an independent risk factor for colon cancer, facilitating colon cancer incidence, and affecting its recurrence, metastasis and prognosis (6,7). Our previous study revealed that patients with colon cancer and diabetes had a higher risk of recurrence after surgery than those without diabetes (8). However, the mechanisms by which hyperglycemia mediates poor prognosis in CRC remain unclear. Exploring the link between hyperglycemia and colon cancer will improve the understanding of cancer pathogenesis, while offering a more valuable guide for personalized treatment of colon tumors in diabetic patients.

Tribble (TRIB) pseudokinases control multiple aspects of eukaryotic cell biology and have evolved unique features that distinguish them from other protein kinases (9). The TRIB family comprises TRIB1, TRIB2 and TRIB3, and it has been suggested that TRIB3 serves a crucial role in diabetes, malignancy and cardiovascular diseases (10,11). In previous studies, TRIB3 protein levels have been reported to be markedly elevated in gastric, hepatocellular and lung cancer (12-14). However, the role of TRIB3 in colon cancer remains unclear, and its potential to promote colon cancer progression in high-glucose environments is not well understood.

The present study aimed to investigate the expression of TRIB3 in CRC cell lines under high-glucose conditions and in CRC tissues from patients with diabetes. Furthermore, the study aimed to explore whether TRIB3 regulates the EMT program via the PI3K/AKT pathway to mediate the malignant proliferation and invasion of CRC cells induced by high glucose, and whether suppressing TRIB3 expression could hinder high glucose-induced tumor cell biological behaviors. The findings may aid in the determination of whether targeting

TRIB3 could serve as a potential novel therapeutic strategy for diabetic patients with CRC.

Materials and methods

Cell culture and reagents. The human colorectal adenocarcinoma cell lines HCT116, SW480, DLD-1, and LoVo, and 293T cell lines were purchased from the Academy of Medical Sciences. 293T cells were cultured in DMEM (cat. no. 01-052-1ACS; glucose content, 25 mM; Biological Industries; Sartorius AG); DLD-1 cells were cultured in RPMI-1640 medium (cat. no. PM150110; Procell Life Science & Technology Co., Ltd.); LoVo cells were cultured in Ham's F-12K medium (cat. no. PM150910; Procell Life Science & Technology Co., Ltd.), and HCT116 and SW480 cell lines were cultured in DMEM with different glucose concentrations (including 10, 15, 20, 25, 30, 35 and 40 mM). Media containing different glucose concentrations were prepared by mixing low-glucose DMEM (cat. no. 01-051-1ACS; glucose content, 5 mM; Biological Industries; Sartorius AG) with a condensed glucose solution (1 mM). All culture media contained 10% fetal bovine serum (FBS; cat. no. FSS500; Shanghai ExCell Biology, Inc.) and 1% penicillin-streptomycin compound (cat. no. C0222; Beyotime Biotechnology). All cells were cultivated in a humidified incubator containing 5% CO_2 at 37˚C. For experimental treatment, LY294002 (cat. no. S1105; Selleck Chemicals) was diluted with high-glucose DMEM to a final working concentration of 10 μM, and CRC or transfected CRC cells were treated with this working solution at 37˚C for 24 h.

Short hairpin RNA (shRNA)-mediated knockdown of TRIB3. The human TRIB3 shRNA lentiviral vector [YSH-LV001-hTRIB3(shRNA), EGFP/puro] and the control lentiviral vector (YSH-LV001-Ctrl) were purchased from Ubigene. A third-generation lentiviral packaging system was used. Lentiviruses were produced by transfecting 293T cells in 10 cm dishes with a total of 20 μg plasmids encoding psPAX2, pMD2.G and lentiviral vectors at a ratio of transfer plasmid/packaging plasmid/envelope plasmid of 4:3:1. Transfection was performed using Lipofectamine® 3000 (Invitrogen; Thermo Fisher Scientific, Inc.) for 6 h at 37˚C in a humidified 5% CO_2 incubator. Lentiviral supernatants were collected at 48 and 72 h post-transfection, filtered through a 0.45-μm filter, and concentrated if needed. CRC cells were then transduced with lentivirus particles at a multiplicity of infection of 10 in the presence of 5 μg/ml polybrene (cat. no. C0351; Beyotime Biotechnology) for 24 h before the medium was replaced. The infected CRC cells were cultured for an additional 72 h before puromycin selection or subsequent experiments. Stably transduced cells were selected with 2 μg/ml puromycin (cat. no. ST551; Beyotime Biotechnology) and subsequently maintained in medium containing 1 μg/ml puromycin.

Transwell migration and invasion assays. Prior to the migration and invasion assays, HCT116, SW480, DLD1 and LoVo cell lines were subjected to TRIB3 knockdown, and HCT116 and SW480 cells were treated with LY294002 as aforementioned. Cells were cultured under low glucose (10 mM), control glucose (25 mM) and high glucose (40 mM) conditions according to the corresponding experimental requirements. For the migration assay, $5x10^4$ cells/well suspended in serum-free medium were inoculated into the upper chamber of a 24-well Transwell system (8.0 μm pore polycarbonate membrane). For invasion assays, the upper chambers were precoated with a 1:8 mixture of reduced growth factor Matrigel (Corning, Inc.) and PBS, followed by incubation at 37˚C for 2 h before cell inoculation. The lower chambers were filled with complete medium containing 10% FBS as a chemoattractant. After incubation at 37˚C for 24 h, the migrating cells at the bottom were fixed with 4% paraformaldehyde at room temperature for 15 min, followed by staining with 0.1% crystal violet at room temperature for 10-15 min. Using a light microscope, 3-5 fields/wells were selected for cell counting.

Nuclear protein isolation. For nuclear protein isolation, CRC cells cultured under normal or high glucose conditions were harvested by scraping and centrifugation at 1,000 x g for 5 min at 4˚C. Nuclear proteins were extracted using a Nuclear and Cytoplasmic Protein Extraction Kit (cat. no. P0027; Beyotime Biotechnology). Briefly, cell pellets were resuspended in ice-cold Cytoplasmic Extraction Buffer A supplemented with 1 mM phenylmethylsulfonyl fluoride (PMSF), vortexed thoroughly, and incubated on ice for 15 min. After adding Cytoplasmic Extraction Buffer B and brief vortexing, samples were centrifuged at 12,000 x g for 5 min at 4˚C, and the cytoplasmic fraction was discarded. The nuclear pellet was resuspended in ice-cold Nuclear Extraction Buffer supplemented with 1 mM PMSF, incubated on ice for 30 min with vigorous vortexing for 15 sec every 2 min to lyse the nuclear membrane. Finally, nuclear lysates were centrifuged at 12,000 x g for 15 min at 4˚C, and the supernatant was collected and stored at -80˚C.

Protein extraction and western blotting. Whole-cell protein extraction was performed using RIPA lysis buffer (cat. no. R00010; Beijing Solarbio Science & Technology Co., Ltd.) and protein concentration was quantified using a BCA protein detection kit (Thermo Fisher Scientific, Inc.). Subsequently, proteins (40 μg/lane) were denatured and separated by SDS-PAGE on 10% gels. The proteins were then transferred onto PVDF membranes (MilliporeSigma) using a semi-dry method at a current of 200 mA for a duration of 1.5 h. Membranes were blocked with 8% non-fat milk at room temperature (25˚C) for 1 h with constant gentle shaking. After overnight incubation with primary antibodies at 4˚C, the membranes were incubated for 1 h at room temperature with horseradish peroxidase (HRP)-conjugated secondary goat anti-rabbit or anti-mouse-polyclonal immunoglobulin G antibodies. Signals were visualized using an enhanced chemiluminescence kit (Applygen Technologies, Inc.). For semi-quantitative analysis of the results, ImageJ 1.46r software (National Institutes of Health) was used. Detailed information regarding all antibodies used in the present study is provided in Table SI.

RNA extraction and reverse transcription-quantitative (RT-qPCR). Total RNA was extracted from the cells using TRIeasy™ reagent (cat. no. 10606ES60; Shanghai Yeasen Biotechnology Co., Ltd.) according to the manufacturer's

instructions. Utilizing 1 μg total RNA, cDNA was synthesized in a 20-μl RT reaction using Hifair® II 1st Strand cDNA Synthesis SuperMix (cat. no. 11137ES60; Shanghai Yeasen Biotechnology Co., Ltd.) according to the manufacturer's protocol. To assess the mRNA expression levels of TRIB3 and EMT markers, qPCR analysis was conducted using a 7500 Sequence Detection System (Applied Biosystems; Thermo Fisher Scientific, Inc.) and the SYBR Green Premix (cat. no. 11203ES; Shanghai Yeasen Biotechnology Co., Ltd.) under the following conditions: Initial denaturation at 95˚C for 30 sec, followed by 40 cycles of 95˚C for 10 sec and 60˚C for 30 sec, with a subsequent melting curve analysis. The primer sequences are listed in Table SII. All experiments were conducted in triplicate to ensure consistency and reliability. mRNA expression levels were quantified using the $2^{-\Delta\Delta Cq}$ method after normalization to β-actin (15).

Cell proliferation assay. Cells were seeded in 96-well plates at a density of $5x10^3$ cells in 100 μl medium/well 1 day before the experiment. At different time points (0, 6, 24 and 48 h), medium containing 10% Cell Counting Kit-8 (CCK-8; cat. no. CK001-500T; Beijing LABLEAD Trading Co., Ltd.) was added to each well and the cells were cultured at 37˚C for 1 h. OD was measured at 450 nm using a spectrophotometer.

Immunofluorescence. Special glass cover slides (cat. no. abs7027; Absin Bioscience, Inc.) for cell immunofluorescence were placed in 24-well plates (cat. no. 801006; NEST®; Wuhan NEST Biotechnology Co., Ltd.). SW480 and HCT116 colon cancer cells were seeded at a density of $3x10^4$ cells/well on the glass coverslips. After culturing for 24 h until the cells reached 70% confluence, they were fixed with 4% formaldehyde in PBS for 15 min at room temperature. After blocking with 2% bovine serum albumin (cat. no. 11021029; Gibco; Thermo Fisher Scientific, Inc.) in PBS (PBA) at room temperature for 1 h, the cells were incubated with primary antibodies against E-cadherin (1:150; cat. no. 60335-1-Ig; Proteintech Group, Inc.), vimentin (1:100; cat. no. 10366-1-AP; Proteintech Group, Inc.) and TRIB3 (1:50; cat. no. ab137526; Abcam) in 2% PBA overnight at 4˚C. The cells were then incubated with corresponding secondary antibodies, including FITC-conjugated anti-rabbit (cat. no. SA00003-2; Proteintech Group, Inc.), TRITC-conjugated anti-rabbit (cat. no. SA00007-2; Proteintech Group, Inc.), FITC-conjugated anti-mouse (cat. no. SA00003-1; Proteintech Group, Inc.) and TRITC-conjugated anti-mouse (cat. no. SA00007-1; Proteintech Group, Inc.), and counterstained with DAPI (cat. no. ZLI-9557; Beijing Zhongshan Jinqiao Biotechnology Co., Ltd.). Images were captured and analyzed using fluorescence microscopy.

Immunohistochemistry. Pathological tissues were obtained from the surgical samples of patients with colon cancer at Beijing Chaoyang Hospital affiliated with Capital Medical University (Beijing, China) between January 2019 and December 2021. The inclusion criteria included pathologically confirmed colon cancer, with complete clinicopathological data and no preoperative neoadjuvant therapy; the exclusion criteria included concurrent other malignancies, severe systemic diseases, poor tissue quality or lost follow-up. The study was approved by the Ethics Committee of Beijing Chaoyang Hospital affiliated with Capital Medical University. Tumor staging was determined according to the TNM staging system, and the detailed clinicopathological information of the patients is provided in Table SIII (16). Tissues were fixed in 4% formalin for 24-48 h at room temperature and then embedded in paraffin at 58-60˚C for ~10 min. Tissue specimens, each at a thickness of 4 μm, were then subjected to deparaffinization and hydration. Deparaffinization was performed with xylene (three changes, 5 min each), followed by sequential hydration with a gradient ethanol series (100, 95, 85 and 75%, 3 min each) and a final rinse with distilled water. Subsequently, heat-induced epitope retrieval was performed in a pressure cooker with 0.01 mol/l citrate buffer (pH 6.0) for 30 min. The sections were then treated with 3% hydrogen peroxide for 15 min at room temperature to block endogenous peroxidase activity, followed by blocking with 5% goat serum (cat. no. 16210064; Gibco; Thermo Fisher Scientific, Inc.) for 30 min at room temperature. Subsequently, the sections were incubated overnight at 4˚C with TRIB3 antibody (1:400; cat. no. ab137526; Abcam), followed by incubation with HRP-conjugated goat anti-rabbit secondary antibody (1:500; cat. no. SA00001-2; Proteintech Group, Inc.) for 1 h at room temperature. Immunolabeling was performed using a DAB detection kit (cat. no. ZLI-9019; Beijing Zhongshan Jinqiao Biotechnology Co., Ltd.). Following a 10-mi rinse in water, the sections were re-stained with 0.5% hematoxylin (cat. no. ZLI-9609; OriGene Technologies, Inc.) for 1.5 min at room temperature. Immunohistochemical signals were captured using an optical microscope (Olympus Corporation). Staining intensity was scored as 0 (negative), 1 (weak), 2 (moderate) and 3 (strong). The percentage of positive cells was scored as 0 (0%), 1 (1-25%), 2 (26-50%), 3 (51-75%) and 4 (76-100%). The final IHC score was calculated by multiplying the intensity score by the percentage score, ranging from 0 to 12.

In vivo subcutaneous tumor formation assay. Cell suspensions of HCT116/Ctrl and HCT116/shTRIB3 cells were prepared, with the density adjusted to $5x10^7$ cells/ml. Briefly, 5-week-old female BALB/c nude mice (weight: 18-22 g; n=5/subgroup; total, 20 mice; no significant difference in body weight among groups before the experiment) were purchased from Beijing Vital River Laboratory Animal Technology Co., Ltd. The mice were divided into four groups to be subcutaneously injected with tumor cells into the right inguinal region: Two groups injected with HCT116/Ctrl cells and two groups injected with HCT116/shTRIB3 cells. Each mouse received a 100-μl cell suspension, corresponding to $5x10^6$ cells/mouse. The HCT116/Ctrl and HCT116/shTRIB3 groups were each divided into two subgroups receiving either normal drinking water or 30% high-sugar water [as recommended in multiple studies (17,18)]. Mice were housed in cages with a controlled temperature (22±2˚C) and relative humidity (40-60%) under a 12-h light/dark cycle throughout the study. All mice had unrestricted access to a standard diet (crude protein 16%, crude fat 4%, crude fiber 12% and ash 8%) and had free access to normal or 30% high-sugar water as assigned. Tumor size was measured every 5 days. Tumor volume was calculated using the formula: Volume (mm^3)=(length x $width^2$)/2.

Mice were euthanized by CO_2 inhalation 21 days after tumor implantation. The maximum tumor diameter did not

exceed 12 mm, the tumors showed no signs of ulceration and mice exhibited good general health with no signs of cachexia. Briefly, CO_2 was introduced at a displacement rate of 30% chamber volume/min, in accordance with the AVMA Guidelines for the Euthanasia of Animals (19). Confirmation of death required verifying that the mouse was motionless and exhibited no respiratory activity; after turning off the CO_2, the mice were monitored for an additional 2-3 min to verify death.

The Cancer Genome Atlas (TCGA) data. The mRNA expression data of TRIB3 (RNAseq) from 430 patients with CRC in TCGA database (cohort: TCGA CRC) were collected from UCSC Xena (http://xena.ucsc.edu/) to examine the differences in TRIB3 expression between tumor and adjacent non-tumor tissues. To investigate the correlation between TRIB3 and the PI3K/AKT pathway, the 'ggcorrplot' R package (version 0.1.4.1; http://www.sthda.com/english/wiki/ggcorrplot-visualization-of-a-correlation-matrix-using-ggplot2) was used to plot the correlation heat map, and the cor() function was used to calculate the Spearman correlation coefficient. The R software used in the present study was R version 4.5.1 (R Foundation for Statistical Computing; https://www.r-project.org/).

Statistical analysis. Data analysis was performed using GraphPad Prism software (version 6.0; Dotmatics). Unpaired student's t-test was used to assess statistical differences for parametric analyses. For non-parametric comparisons, the Mann-Whitney U test was used. Multiple group comparisons were analyzed one-way ANOVA, with inter-group differences further delineated by Tukey's post hoc test. Quantitative data are presented as the mean ± standard deviation, with all experiments conducted in triplicate to ensure consistency and reliability. $P<0.05$ was considered to indicate a statistically significant difference.

Results

High glucose activates the malignant behavior of CRC cells. To validate whether high glucose levels promote tumor development, a series of *in vitro* assays were conducted to examine the effects of high-glucose levels on CRC cell functions. Emerging research has revealed that when selecting 2 g/l (11.1 mM) and 5 g/l (27.8 mM) as low- and high-glucose concentrations, respectively, two standards are satisfied: i) Cell viability is >80% and ii) the apoptosis rate is <10% (20). To expand the concentration differences, in the current study, 10 and 40 were we selected as the low- and high-glucose concentrations, respectively.

Colon tumor cells were cultured in gradient glucose conditions (10-40 mM) for 48 h and the proliferative ability of the two CRC cell lines, SW480 and HCT116, was assessed using the CCK-8 assay. Compared with in cells treated with low glucose (10 mM glucose), cells treated with high glucose (40 mM glucose) exhibited a significantly higher proliferative potential (Fig. 1A). To investigate the effect of high-glucose levels on the migratory and invasive potential of CRC cells, Transwell assays were performed. The findings revealed that CRC cells exposed to high-glucose levels exhibited increased invasion and migration compared with those exposed to low-glucose levels (Fig. 1B). Alterations in cancer cell migration and invasion capacity are commonly linked to epithelial-mesenchymal transition (EMT). Therefore, the expression levels of EMT-related markers were detected, including the epithelial markers E-cadherin and ZO1, and the mesenchymal markers N-cadherin, Vimentin and Snail. RT-qPCR results showed a significant increase in the expression levels of N-cadherin, Vimentin and Snail, and a reduction in the expression of E-cadherin and ZO1 in CRC cells in response to a high-glucose concentration (Fig. 1C). Subsequently, these findings were corroborated by western blotting and immunofluorescence staining, which consistently obtained similar results (Fig. 1D and E). These findings indicated that high-glucose levels may induce tumorigenesis and EMT in CRC cells.

High glucose induces TRIB3 expression in CRC. To verify the relationship between high-glucose levels and TRIB3, the mRNA and protein expression levels of TRIB3 were measured in CRC cells treated with the indicated glucose concentrations. RT-qPCR results showed that with an increase in glucose concentration, the expression of TRIB3 exhibited a gradual upward trend (Fig. 2A). Western blotting also revealed an apparent increase in TRIB3 protein levels after treatment with HG compared with LG; in response to a 40-mM glucose concentration, the expression of TRIB3 was approximately three times higher than that in the group treated with 10 mM glucose (Fig. 2B). Immunofluorescence staining provided corroborative evidence (Fig. 2C). As shown in the representative immunohistochemistry images, TRIB3 protein levels in patients with diabetes and CRC were higher than those in patients with CRC without diabetes (Fig. 2D). Notably, TRIB3 expression was markedly elevated at the cellular level under conditions of high-glucose exposure, and this upregulation was also prominent in patients with CRC and concurrent diabetes.

TRIB3 knockdown suppresses the proliferation, invasion and EMT process of CRC cells. The expression levels of TRIB3 were detected in SW480, HCT116, DLD-1 and LoVo cells (Figs. 3A and S1A). To verify whether TRIB3 mediates the malignant phenotype of CRC cells, stable TRIB3 knockdown clones were constructed: SW480/shTRIB3, HCT116/shTRIB3, DLD-1/shTRIB3 and LoVo/shTRIB3, and knockdown efficiency was confirmed by western blotting (Figs. 3B and S1B). Notably, CRC cells transduced with shTRIB3 exhibited significantly decreased proliferation, as determined by the CCK-8 assay (Figs. 3C and S1C). To investigate the influence of TRIB3 on the migratory and invasive potential of CRC cells, Transwell assays were performed and the results revealed that shTRIB3-transduced CRC cells exhibited decreased invasion and migration compared with that in the control groups (Figs. 3D and S1D). Subsequently, the effects of TRIB3 knockdown on the expression levels of EMT markers were assessed using RT-qPCR. Compared with in the control group, an increase in the expression levels of E-cadherin and ZO1, alongside a decrease in the levels of N-cadherin and Vimentin, were observed in shTRIB3-transduced CRC cells (Fig. 3E). Furthermore, similar results were obtained by western blotting (Fig. 3F). These results suggest that TRIB3 has the potential to

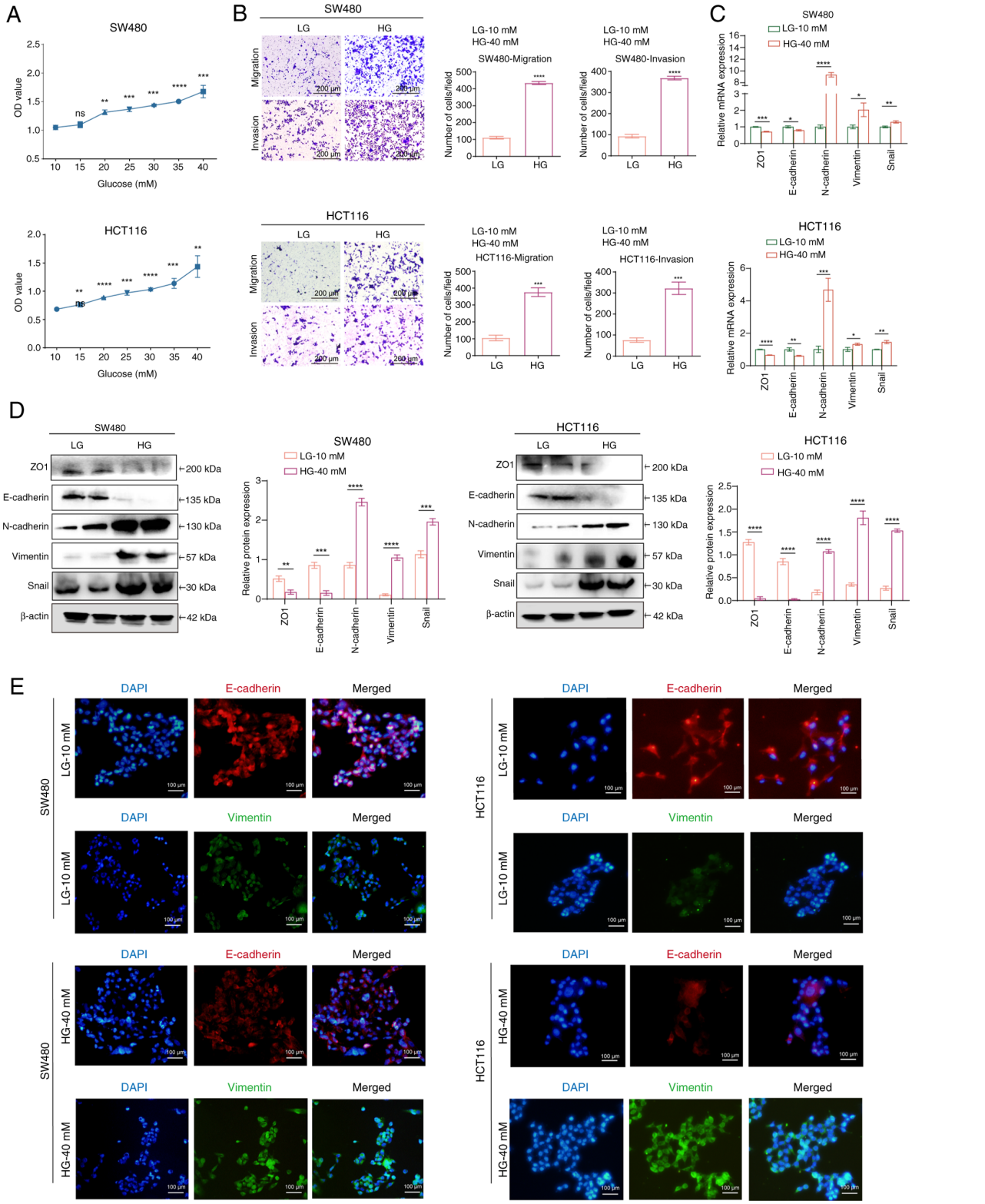

Figure 1. HG induces tumorigenesis and EMT in CRC cells. (A) Cell Counting Kit-8 assay was performed to examine the effects of a gradient glucose concentration within 48 h on the proliferation of two CRC cell lines, SW480 and HCT116. **P<0.01, ***P<0.001, ****P<0.0001 vs. 0 mM glucose group. (B) Transwell assays were performed to evaluate the effects of LG and HG on the migration and invasion of CRC cells. ***P<0.001, ****P<0.0001 vs. LG group. (C) Reverse transcription-quantitative PCR examination of EMT markers after CRC cells were treated with LG or HG for 48 h. (D) Western blotting was utilized to evaluate the levels of EMT marker proteins following treatment of CRC cells with either LG or HG for 48 h. *P<0.05, **P<0.01, ***P<0.001, ****P<0.0001 vs. LG group. (E) Immunofluorescence staining of E-cadherin and Vimentin in two CRC cell lines treated with LG or HG for 48 h. For all bar-plots, data are presented as the mean ± SEM, n=3. CRC, colorectal cancer; EMT, epithelial-mesenchymal transition; HG, high glucose; LG, low glucose; ns, not significant.

promote the malignant behavior of CRC cells and drive EMT in tumor cells. However, whether TRIB3 serves as a key molecule driving the augmented malignant capabilities in the high-glucose environment of CRC remains unknown.

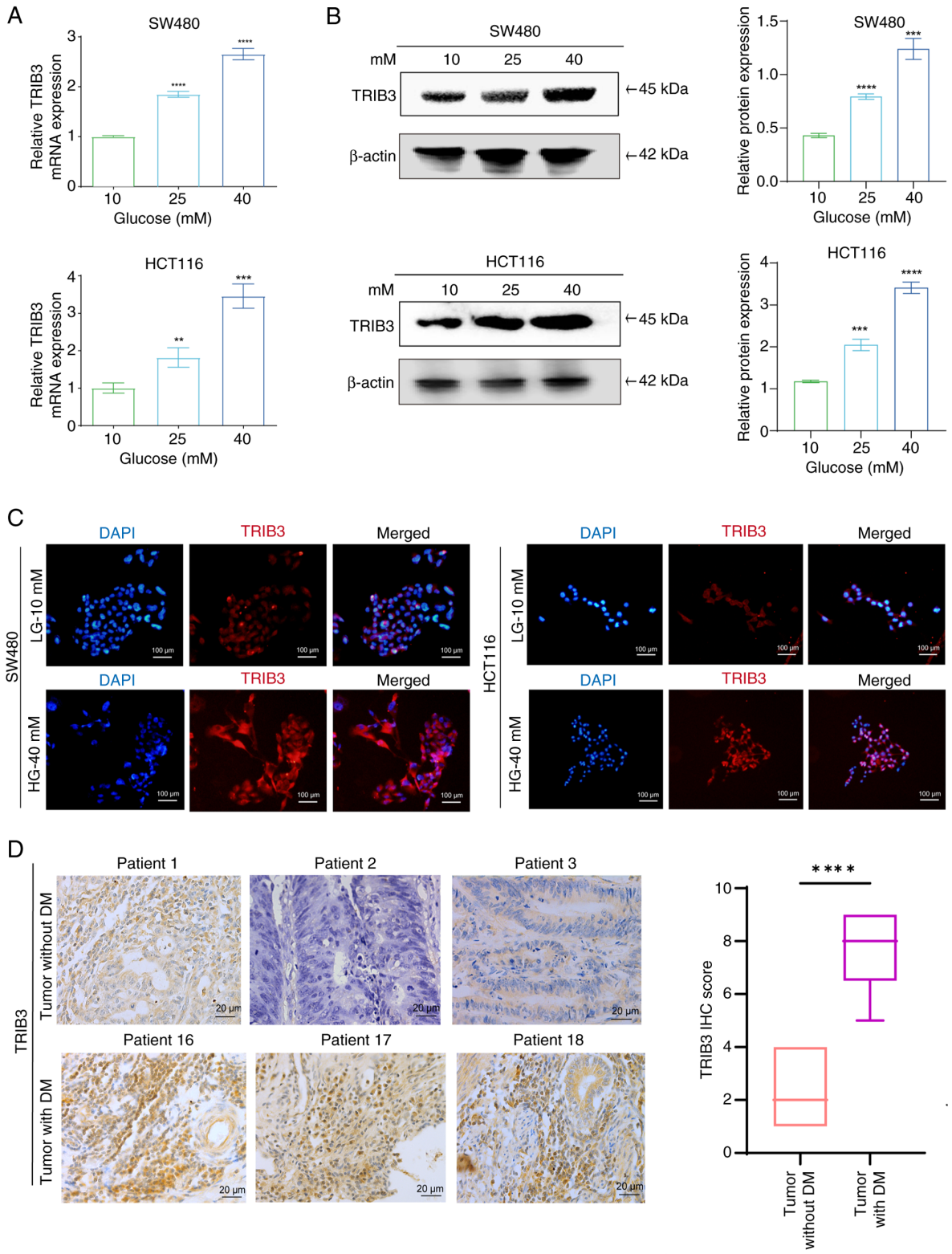

Figure 2. HG activates TRIB3 expression in CRC. (A) Reverse transcription-quantitative PCR was conducted to analyze the mRNA expression levels of TRIB3 in CRC cells subjected to varying glucose concentrations. (B) Western blot analysis to detect the protein expression levels of TRIB3 in CRC cells treated with a gradient of glucose concentrations. **P<0.01, ***P<0.001, ****P<0.0001 vs. 10 mM glucose group. (C) Immunofluorescence staining of TRIB3 expression in CRC cells exposed to HG or LG concentrations for 48 h. (D) Representative IHC images of TRIB3 protein levels from patients with CRC with or without DM stratified by IHC score. ****P<0.0001. Data are presented as the (A-C) the mean ± SEM, n=3; or (D) median (interquartile range), CRC, colorectal cancer; DM, diabetes mellitus; HG, high glucose; IHC, immunohistochemistry; LG, low glucose; TRIB3, tribbles 3.

TRIB3 promotes high glucose-induced malignancy in CRC cells. To validate the role of TRIB3 in promoting malignancy under high-glucose conditions, a CCK-8 assay was performed. The results demonstrated that glucose-induced CRC cell proliferation was significantly reduced by TRIB3 knockdown (Fig. 4A). In addition, Transwell assay results showed that

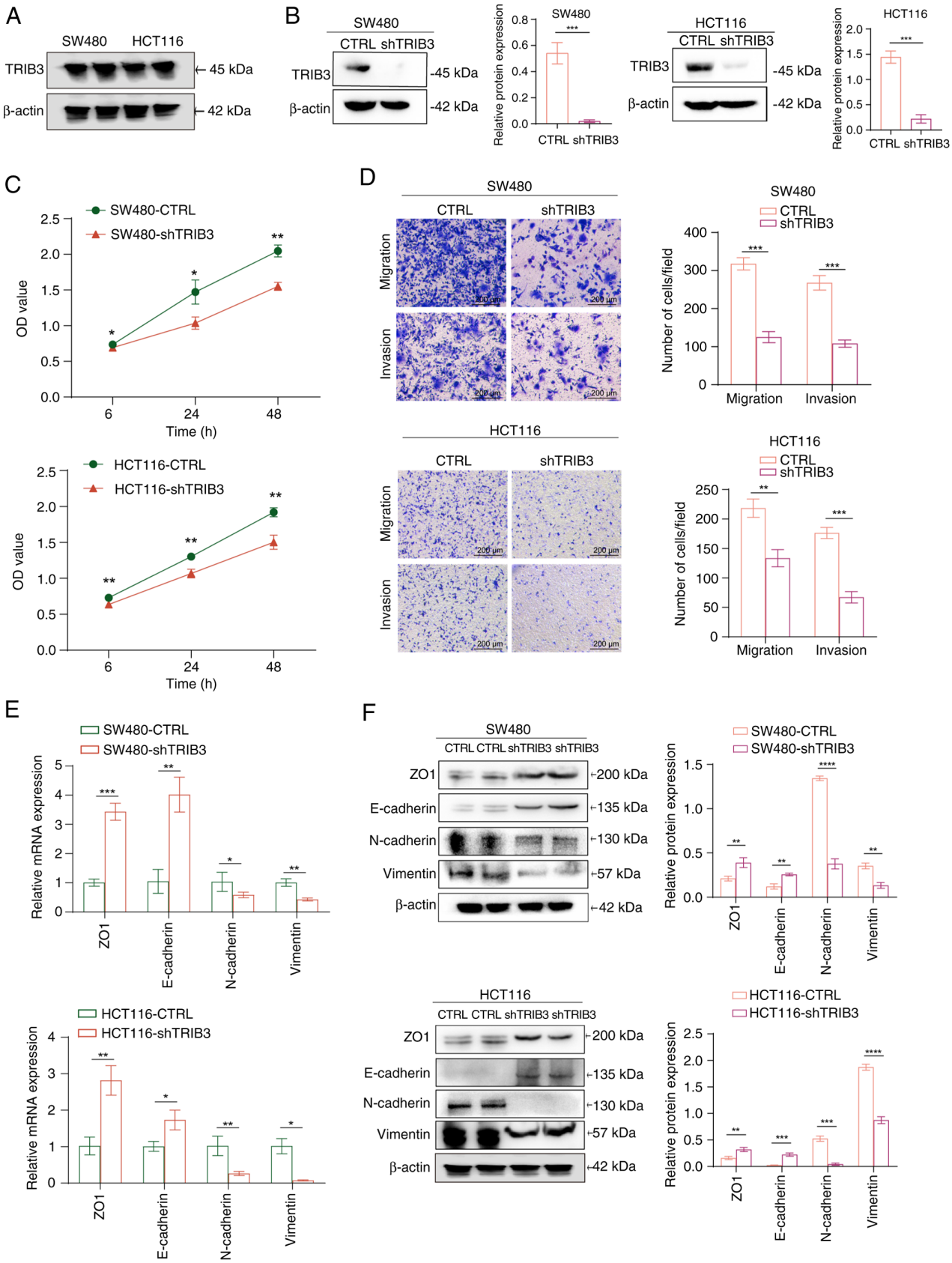

Figure 3. TRIB3 mediates the proliferation and invasiveness of CRC cells by remodeling the EMT process. (A) Western blotting was performed to evaluate the protein expression levels of TRIB3 in the CRC cell lines SW480 and HCT116. (B) Western blotting validation of TRIB3 knockdown in two cancer cell lines. ***P<0.001. (C) Cell counting kit-8 assay was used to investigate the impact of TRIB3 knockdown on the proliferation of two CRC cell lines. *P<0.05, **P<0.01, vs. control group. (D) Transwell assays were performed to evaluate the changes in cell migration and invasion induced by TRIB3 knockdown in two cancer cell lines. (E) Reverse transcription-quantitative PCR was used to examine the impact of TRIB3 knockdown on the mRNA expression levels of EMT markers. (F) Western blotting was utilized to evaluate the impact of TRIB3 knockdown on the protein expression levels of EMT markers. *P<0.05, **P<0.01, ***P<0.001, ****P<0.0001. For all bar-plots, data are presented as the mean ± SEM, n=3. CRC, colorectal cancer; CTRL, control; EMT, epithelial-mesenchymal transition; sh, short hairpin; TRIB3, tribbles 3.

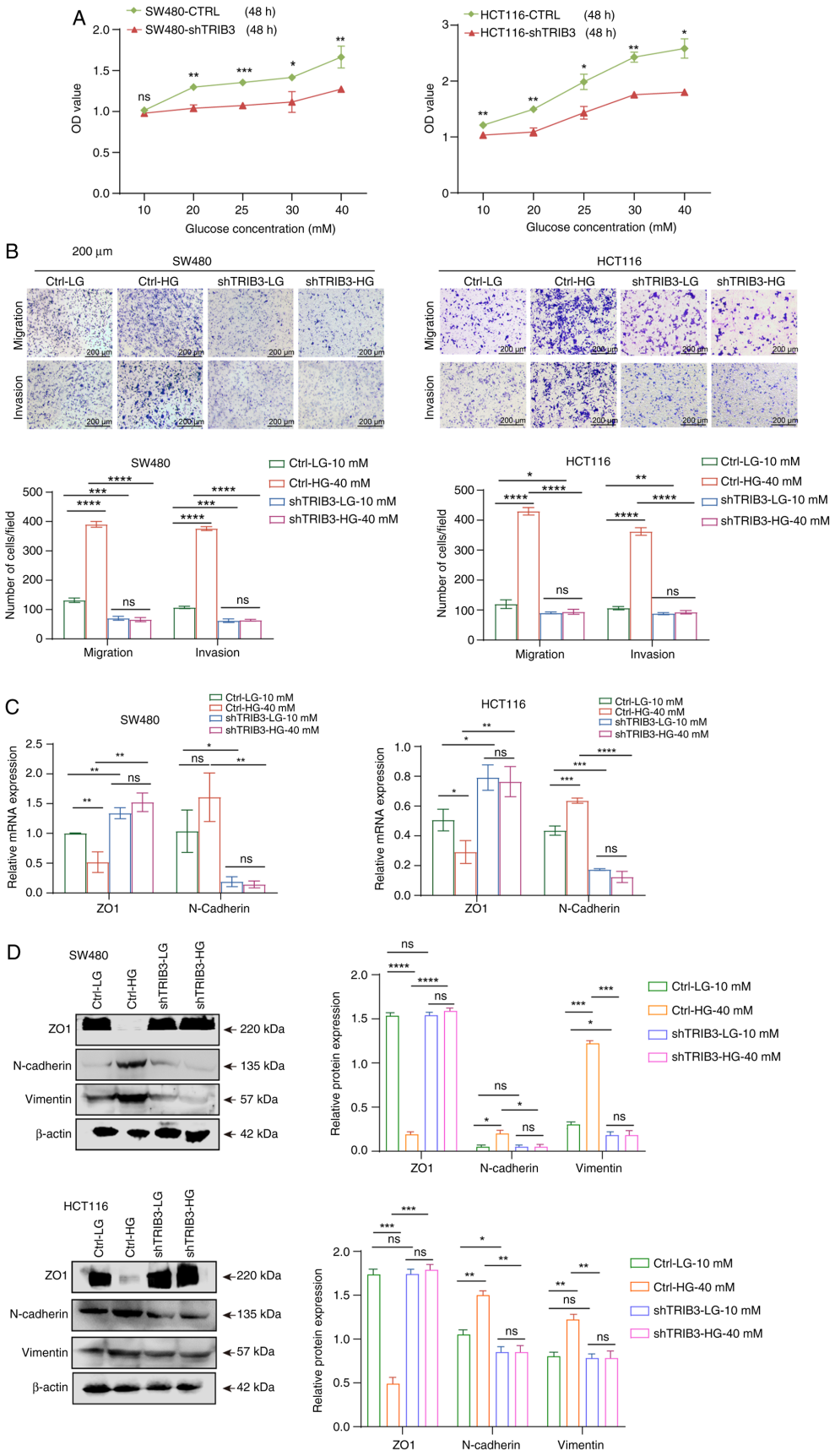

Figure 4. Knockdown of TRIB3 alleviates HG-induced malignancy and EMT in CRC cells. (A) Cell counting kit-8 assay was performed to evaluate the effects of TRIB3 knockdown on CRC cell proliferation induced by different glucose concentrations. *P<0.05, **P<0.01, ***P<0.001 vs. control group. (B) Transwell assays were used to assess the effects of TRIB3 knockdown on the invasive and migratory capabilities of CRC cells under HG conditions. (C) Reverse transcription-quantitative PCR was performed to evaluate the effects of shTRIB3 on HG-induced EMT in two cancer cell lines (SW480 and HCT116). (D) Western blotting was used to assess the changes in the expression of EMT molecules upon TRIB3 knockdown in a HG environment. *P<0.05, **P<0.01, ***P<0.001, ****P<0.0001. For all bar-plots, data are presented as the mean ± SEM, n=3. CRC, colorectal cancer; CTRL, control; EMT, epithelial-mesenchymal transition; HG, high glucose; LG, low glucose; ns, not significant; sh, short hairpin; TRIB3, tribbles 3.

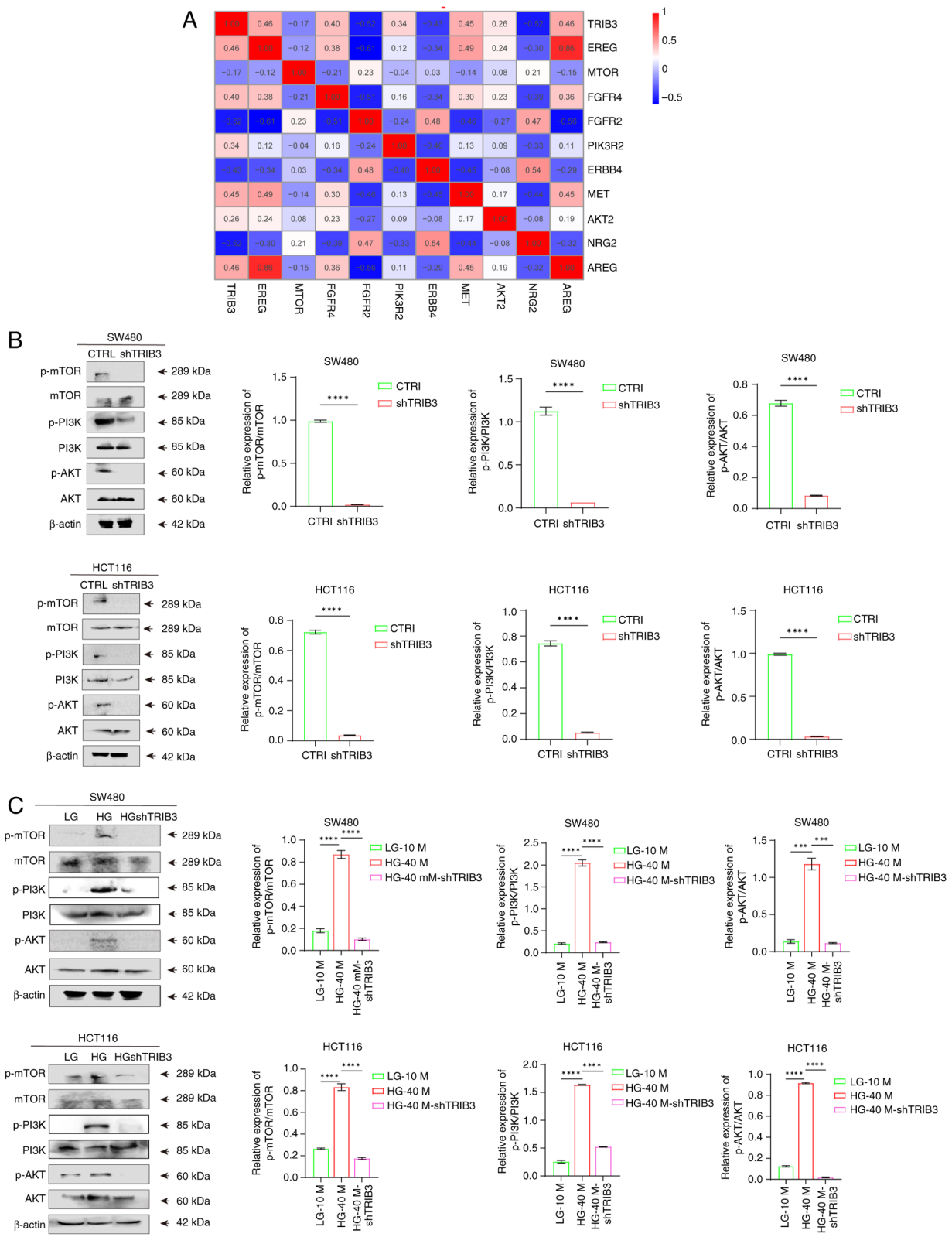

Figure 5. TRIB3 activates the PI3K/AKT signaling pathway in high glucose in colorectal cancer cells. (A) Heatmap analysis demonstrating the correlation between TRIB3 expression levels and PI3K-related pathway. (B) Western blotting was utilized to evaluate the impact of TRIB3 knockdown on the PI3K/AKT pathway activation status. (C) Western blotting was utilized to evaluate the alterations in the PI3K/AKT pathway activation status following TRIB3 knockdown under HG conditions. ***P<0.001, ****P<0.0001. For all bar-plots, data are presented as the mean ± SEM, n=3. CTRL, control; HG, high glucose; LG, low glucose; ns, not significant; p-, phosphorylated; sh, short hairpin; TRIB3, tribbles 3.

TRIB3 knockdown reversed the phenotype of migration and invasion induced by high glucose in CRC cells (Fig. 4B). To validate whether the knockdown of TRIB3 could alleviate high glucose-induced EMT in CRC cells, RT-qPCR was used to assess the expression levels of EMT markers; the results revealed that the knockdown of TRIB3 reversed the trend of

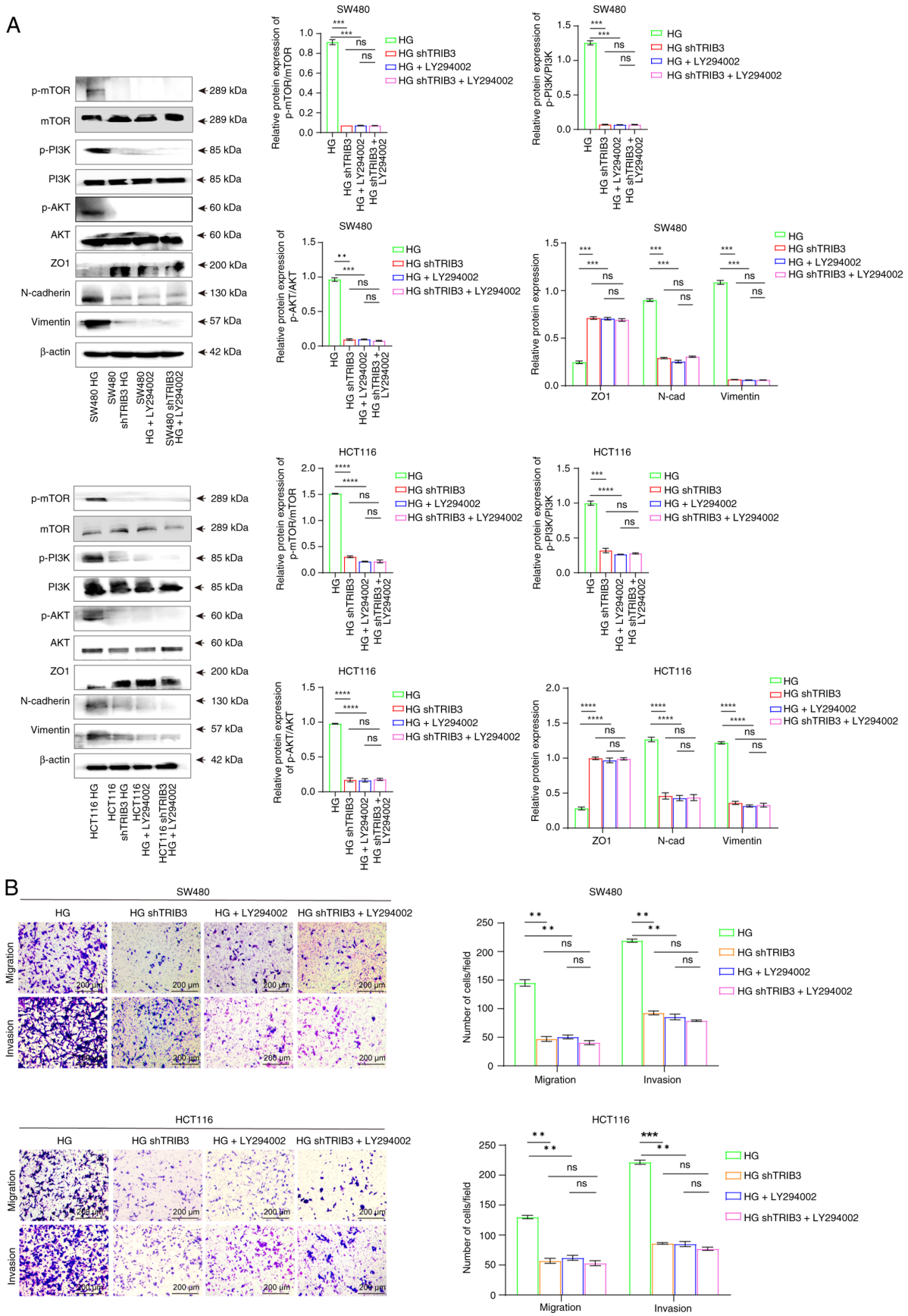

Figure 6. TRIB3 promotes malignant behavior of colorectal cancer cells through the PI3K/AKT pathway. (A) Western blot analysis was performed to evaluate the levels of epithelial-mesenchymal transition-related proteins and PI3K/AKT/mTOR pathway proteins in cells treated with the PI3K/AKT/mTOR pathway inhibitor LY294002 (10 μM), both in the presence and absence of shTRIB3 in HG conditions. (B) Transwell assays were used to evaluate the changes in cell migration and invasion induced by inhibition of the PI3K/AKT signaling pathway under HG conditions, with or without TRIB3 knockdown. **P<0.01, ***P<0.001, ****P<0.0001. For all bar-plots, data are presented as the mean ± SEM, n=3. HG, high glucose; ns, not significant; p-, phosphorylated; sh, short hairpin; TRIB3, tribbles 3.

HG-induced exacerbation of EMT, as indicated by the expression levels of ZO-1 and N-cadherin (Fig. 4C). Furthermore, these observations were corroborated by western blot analysis, which revealed that inhibiting TRIB3 in a high-glucose environment resulted in a marked increase in the expression levels of the epithelial marker ZO1. Furthermore, the expression levels of mesenchymal markers, including N-cadherin and Vimentin, were markedly decreased (Fig. 4D).

To further validate the aforementioned conclusions *in vivo*, HCT116 control and HCT116 shTRIB3 cells were subcutaneously inoculated into mice. The HCT116 control group was divided into two subgroups receiving either normal drinking water or 30% high-sugar water, with the same treatment applied to the HCT116 shTRIB3 group. Notably, subcutaneous tumors formed exclusively in the HCT116 groups, whereas almost no tumors were observed in the TRIB3-knockdown groups (Fig. S2). Moreover, the subcutaneous tumor formation in the high-sugar drinking group was significantly enhanced compared with that that in the normal drinking water group. Notably, these *in vivo* data confirmed that TRIB3 knockdown can markedly impair cell tumorigenicity, which is also consistent with the *in vitro* experimental results, confirming the driving role of TRIB3 in tumor formation. However, its significant upregulation under high-glucose conditions further exacerbates its regulatory impact on the malignant progression of tumors (Fig. S2). These findings illustrate that TRIB3 serves a pivotal role in amplifying the proliferative and invasive capabilities of CRC cells in a high-glucose environment. However, the mechanism by which TRIB3 activates the EMT remains unclear.

TRIB3 induces activation of the PI3K/AKT signaling pathway under high-glucose conditions in CRC cells. Based on TCGA-Colon Adenocarcinoma dataset, it was revealed that TRIB3 was closely associated with the PI3K/AKT pathway in patients with CRC, as evidenced by the increased expression of PI3K/AKT pathway-related activation markers (AREG, AKT2, MET, PIK3R2, FGFR2, and EREG) (Fig. 5A). Since the PI3K/AKT pathway is crucial for cancer cell proliferation and metastasis, the phosphorylation of proteins in the PI3K pathway was evaluated in cells under normal glucose conditions and in shTRIB3 CRC cells by western blotting. The western blotting findings revealed a marked reduction in PI3K, AKT and mTOR phosphorylation levels in SW480 and HCT116 cell lines upon TRIB3 knockdown compared with in the control groups, without notably altering the total PI3K, AKT and mTOR expression levels (Fig. 5B). Furthermore, an apparent increase in p-AKT, p-PI3K and p-mTOR levels was detected after treatment with a high-glucose concentration compared with that in the low-glucose concentration group, whereas TRIB3 knockdown significantly inhibited this phosphorylation (Fig. 5C). In summary, TRIB3 may activate the PI3K/AKT pathway in response to high glucose levels.

High glucose-induced TRIB3 activation drives CRC malignancy via the PI3K/AKT pathway. To investigate whether TRIB3 drives malignant progression in CRC cells under high-glucose conditions via PI3K/AKT pathway activation, the PI3K/AKT/mTOR pathway was first inhibited using LY294002 (10 μM) and then TRIB3 was knocked down. In high-glucose environments, LY294002 treatment alone led to decreased phosphorylation levels of PI3K, AKT and mTOR, accompanied by elevated ZO1 expression and reduced N-cadherin/Vimentin expression compared with that in the high-glucose control group (Fig. 6A). Notably, TRIB3 knockdown following pathway inhibition did not further enhance these effects, indicating that they act on the same regulatory axis. Furthermore, Transwell assays revealed that LY294002 treatment under high-glucose conditions significantly impaired the invasion and migration of CRC cells compared with that in the high-glucose control group, and TRIB3 knockdown elicited identical phenotypic effects (Fig. 6B). These findings suggest that TRIB3-driven invasion and migration under high-glucose conditions are predominantly mediated by the PI3K/AKT signaling pathway.

In order to confirm the interaction, the western blot analysis showed that TRIB3 depletion not only reduced PI3K/AKT phosphorylation but also inhibited GSK-3β phosphorylation at Ser9, which in turn led to increased β-catenin phosphorylation and its subsequent degradation in the cytoplasm (Fig. S3A and B). This reduction in cytoplasmic β-catenin stability resulted in decreased nuclear translocation of β-catenin, a phenomenon that may suppress downstream signaling pathways and thereby block tumor progression. These findings further indicated that TRIB3 is a critical molecular driver in the development and progression of CRC, exerting its oncogenic effects by activating multiple signaling pathways. Targeting the TRIB3 pathway presents a potential option for reversing the exacerbated malignant behavior of CRC cells induced by a high-glucose environment.

Discussion

Due to alterations in diet and lifestyle, such as increased consumption of high-fat, high-calorie food, insufficient physical activity and smoking, the prevalence of CRC and diabetes is likely to increase (21-23). Notably, evidence has indicated an association between diabetes and various types of cancer, including breast, pancreatic and liver cancer (24-26), and type 2 diabetes has been associated with a higher risk of CRC in an observational study (6). Diabetes exerts a detrimental influence on the outcomes of CRC treatment, resulting in an increased risk of metastasis, recurrence and mortality (7). In our previous study, diabetes was identified as an independent risk factor for postoperative CRC, and diabetic patients with CRC had a higher risk of recurrence (8). However, the mechanism underlying the progression of diabetes into colon cancer remains unclear.

The TRIB3 protein, categorized within the TRIB family of pseudokinases, is characterized by the absence of specific ATP-binding sites and catalytic cores, rendering it devoid of kinase activity (24). Emerging evidence has revealed that, as an intracellular pseudokinase, TRIB3 is a pivotal factor in regulating glucose homeostasis and insulin resistance, and its role as a stress sensor has been firmly established in response to a wide array of stressors, such as hypoxia, fasting and high-glucose levels (27-30).

Numerous studies have uncovered a notable role for TRIB3 in the development of tumors, and TRIB3 has been shown to

be highly expressed in gastric, liver, kidney and non-small cell lung cancer (31,32). Furthermore, TRIB3 upregulation is associated with tumor-related staging, lymph node metastasis, disease recurrence and poor prognosis (33,34). Previous studies have indicated that TRIB3 increases the expression of genes associated with cancer stem cells, including CD44, CD133, OCT4 and SOX2, and facilitates tumor development in CRC, resulting in unfavorable outcomes (2,35,36). Although research has provided information on the role of TRIB3 in patients with CRC and diabetes, the specific underlying mechanisms are yet to be fully elucidated (36). In the current study, the pivotal role of TRIB3 in CRC was not only substantiated, but how TRIB3 facilitates the proliferation, invasion and migration of CRC cells by activating the PI3K/AKT pathway under high-glucose conditions was clarified.

The present study revealed that high-glucose levels could stimulate proliferation, migration, invasion and EMT remodeling in CRC cells, concurrently upregulating the expression of TRIB3. These findings led to the scientific hypothesis that high-glucose levels may facilitate malignant biological phenotypes in CRC through the upregulation of TRIB3. Therefore, in subsequent experiments in a high-glucose environment, TRIB3 was knocked down; the results demonstrated that the suppression of TRIB3 expression significantly counteracted the enhanced cellular proliferation and invasion induced by high-glucose levels, and markedly inhibited activation of the EMT process. These findings strongly support the hypothesis that TRIB3 is a crucial molecule in tumor progression under high-glucose conditions.

Regarding the mechanism by which TRIB3 regulates tumor progression, multiple studies have been conducted. Hua *et al* (35) demonstrated that TRIB3 interacts with β-catenin to promote tumor cell malignancy, which may align with the present findings, as the PI3K/AKT and β-catenin pathways can converge and crosstalk at the GSK-3β site. To confirm this interaction, experiments were performed in CRC cells cultured under high-glucose conditions and with TRIB3 knockdown. The results demonstrated that TRIB3 depletion not only reduced PI3K/AKT phosphorylation but also inhibited GSK-3β phosphorylation at Ser9, leading to increased β-catenin phosphorylation and subsequent degradation in the cytoplasm. This resulted in reduced nuclear translocation of β-catenin, which may suppress downstream signaling pathways and block tumor progression.

Additionally, as demonstrated by Shang *et al* (36), TRIB3 can influence the CRC immune microenvironment and mediate tumor progression by regulating the STAT1-CXCL10 axis. This may be due to factors downstream of the PI3K/AKT pathway, such as NF-κB, which can indirectly regulate STAT1 activity, and TRIB3-mediated inhibition of STAT1 could further impair CXCL10-mediated T-cell recruitment. These findings further indicated that TRIB3 is a critical molecular driver in the development and progression of CRC, exerting its oncogenic effects by activating multiple signaling pathways.

Moreover, numerous studies have explored the mechanisms by which high-glucose levels mediate the upregulation of TRIB3 expression. High-glucose levels are considered to promote glucose metabolism through the hexosamine biosynthetic pathway, which elevates O-GlcNAc-modified proteins. These modified proteins may function as transcription factors or co-regulators that directly or indirectly influence TRIB3 gene expression (37). For example, O-GlcNAc modification of Sp1, a well-known transcription factor, has been shown to upregulate TRIB3 expression (37). In addition, other factors may contribute to high glucose-induced TRIB3 upregulation. For example, high-glucose levels can activate signaling pathways, such as protein kinase C and mitogen-activated protein kinase (38,39). These pathways could regulate TRIB3 expression through the phosphorylation of transcription factors and other regulatory proteins.

In conclusion, multiple studies have suggested that elevated blood glucose levels contribute to the upregulation of TRIB3 expression, and the present study further indicated that the upregulation of TRIB3 expression may activate the PI3K/AKT signaling pathway to promote cell malignant behavior by enhancing EMT. Conversely, TRIB3 knockdown significantly inhibited the PI3K/AKT signaling pathway, thereby suppressing oncogenic signaling and tumor progression. However, the underlying mechanisms remain highly complex and require further investigation in subsequent research. Notably, TRIB3 has emerged as a critical therapeutic target for diabetic CRC.

Acknowledgements

Not applicable.

Funding

This work was supported by the National Natural Science Foundation of China (grant no. 82303649 to RY) and the Natural Science Foundation of Beijing Municipality (grant no. 7232064 to GA).

Availability of data and materials

The data generated in the present study may be requested from the corresponding author.

Authors' contributions

DY conceived and designed the study. RY performed the statistical analysis, revision and final proofreading of the article. YB and XH acquired the data and performed experiments. XH analyzed the data. YG and GA interpreted the data. YB and DY drafted the manuscript. YG and GA revised the manuscript. All authors read and approved the final manuscript. YB and RY confirm the authenticity of all the raw data.

Ethics approval and consent to participate

The use of human tissue samples was approved by the Ethics Committee of Beijing Chaoyang Hospital affiliated with Capital Medical University (approval no. 2020-10-13-4), in accordance with The Declaration of Helsinki and applicable Chinese regulations. Written informed consent was obtained from all the participants for their participation. The animal study protocol was approved by the Animal Ethics Committee of Capital Medical University (approval no. AEE1-2025-1255). The study strictly adhered to the ethical principles and standards set forth by the ethics committee.

Patient consent for publication

All enrolled patients provided written informed consent for publication.

Competing interests

The authors declare that they have no competing interests.

References

1. Harborg S, Kjærgaard KA, Thomsen RW, Borgquist S, Cronin-Fenton D and Hjorth CF: New Horizons: Epidemiology of Obesity, Diabetes Mellitus, and Cancer Prognosis. J Clin Endocrinol Metab 109: 924-935, 2024.
2. Shahid RK, Ahmed S, Le D and Yadav S: Diabetes and cancer: Risk, challenges, management and outcomes. Cancers (Basel) 13: 5735, 2021.
3. Abudawood M: Diabetes and cancer: A comprehensive review. J Res Med Sci 24: 94, 2019.
4. Jordt N, Kjærgaard KA, Thomsen RW, Borgquist S and Cronin-Fenton D: Breast cancer and incidence of type 2 diabetes mellitus: A systematic review and meta-analysis. Breast Cancer Res Treat 202: 11-22, 2023.
5. Blaslov K, Bulum T and Duvnjak L: Pathophysiological factors in the development of diabetic nephropathy-new insights. Acta Med Croatica 68: 135-140, 2014 (In Croatian).
6. Murphy N, Song M, Papadimitriou N, Carreras-Torres R, Langenberg C, Martin RM, Tsilidis KK, Barroso I, Chen J, Frayling TM, *et al*: Associations between glycemic traits and colorectal cancer: A mendelian randomization analysis. J Natl Cancer Inst 114: 740-752, 2022.
7. Roman D, Saftescu S, Timar B, Avram V, Braha A, Negru Ş, Bercea A, Serbulescu M, Popovici D and Timar R: Diabetes mellitus and other predictors for the successful treatment of metastatic colorectal cancer: A retrospective study. Medicina (Kaunas) 58: 872, 2022.
8. Yu D, An G and Yao J: Lymphocyte-to-monocyte ratio combined with CA19-9 for predicting postoperative recurrence of colorectal cancer in patients with diabetes. J Clin Lab Anal 35: e23944, 2021.
9. Eyers PA, Keeshan K and Kannan N: Tribbles in the 21st Century: The evolving roles of tribbles pseudokinases in biology and disease. Trends Cell Biol 27: 284-298, 2017.
10. Lu G, Li J, Gao T, Liu Q, Chen O, Zhang X, Xiao M, Guo Y, Wang J, Tang Y and Gu J: Integration of dietary nutrition and TRIB3 action into diabetes mellitus. Nutr Rev 82: 361-373, 2024.
11. Prudente S, Sesti G, Pandolfi A, Andreozzi F, Consoli A and Trischitta V: The mammalian tribbles homolog TRIB3, glucose homeostasis, and cardiovascular diseases. Endocr Rev 33: 526-546, 2012.
12. Cao X, Fang X, Malik WS, He Y, Li X, Xie M, Sun W, Xu Y and Liu X: TRB3 interacts with ERK and JNK and contributes to the proliferation, apoptosis, and migration of lung adenocarcinoma cells. J Cell Physiol 235: 538-547, 2020.
13. Wang XJ, Li FF, Zhang YJ, Jiang M and Ren WH: TRIB3 promotes hepatocellular carcinoma growth and predicts poor prognosis. Cancer Biomark 29: 307-315, 2020.
14. Yu JJ, Zhou DD, Yang XX, Cui B, Tan FW, Wang J, Li K, Shang S, Zhang C, Lv XX, *et al*: TRIB3-EGFR interaction promotes lung cancer progression and defines a therapeutic target. Nat Commun 11: 3660, 2020.
15. Livak KJ and Schmittgen TD: Analysis of relative gene expression data using real-time quantitative PCR and the 2(-Delta Delta C(T)) Method. Methods 25: 402-408, 2001.
16. Amin MB, Greene FL, Edge SB, Compton CC, Gershenwald JE, Brookland RK, Meyer L, Gress DM, Byrd DR and Winchester DP: The eighth edition AJCC cancer staging manual: Continuing to build a bridge from a population-based to a more 'personalized' approach to cancer staging. CA Cancer J Clin 67: 93-99, 2017.
17. Vaziri-Gohar A, Hue JJ, Abbas A, Graor HJ, Hajihassani O, Zarei M, Titomihelakis G, Feczko J, Rathore M, Chelstowska S, *et al*: Increased glucose availability sensitizes pancreatic cancer to chemotherapy. Nat Commun 14: 3823, 2023.
18. Ding F, Guo Y, Zhang H, Zhong Y, Zhang D, Huang Q, Zheng Z, Liu G, Zhang X and Weng S: High glucose-induced mitochondrial fission drives pancreatic cancer progression through the H3K18la/TTK/BUB1B signal pathway. Cell Signal 135: 112027, 2025.
19. Leary S, Underwood W, Anthony R, Cartner S, Grandin T, Greenacre C, Gwaltney-Bran S, McCrackin MA, Meyer R, Miller D, *et al*: AVMA Guidelines for the Euthanasia of Animals: 2020 Edition. American Veterinary Medical Association, Schaumburg, IL, 2020.
20. Li H, Li C, Zhang B and Jiang H: Lactoferrin suppresses the progression of colon cancer under hyperglycemia by targeting WTAP/m(6)A/NT5DC3/HKDC1 axis. J Transl Med 21: 156, 2023.
21. Sun X, Yan AF, Shi Z, Zhao B, Yan N, Li K, Gao L, Xue H, Peng W, Cheskin LJ and Wang Y: Health consequences of obesity and projected future obesity health burden in China. Obesity (Silver Spring) 30: 1724-1751, 2022.
22. Cignarelli A, Genchi VA, Caruso I, Natalicchio A, Perrini S, Laviola L and Giorgino F: Diabetes and cancer: Pathophysiological fundamentals of a 'dangerous affair'. Diabetes Res Clin Pract 143: 378-388, 2018.
23. Zhan Z, Chen B, Lin W, Chen X, Huang R, Yang C and Guo Z: Rising Burden of colon and rectum cancer in China: An analysis of trends, gender disparities, and projections to 2030. Ann Surg Oncol 32: 3361-3371, 2025.
24. Kang C, LeRoith D and Gallagher EJ: Diabetes, obesity, and breast cancer. Endocrinology 159: 3801-3812, 2018.
25. Norat T, Scoccianti C, Boutron-Ruault MC, Anderson A, Berrino F, Cecchini M, Espina C, Key T, Leitzmann M, Powers H, *et al*: European code against cancer 4th edition: Diet and cancer. Cancer Epidemiol 39 (Suppl 1): S56-S66, 2015.
26. Zhang Z, Qin W and Sun Y: Contribution of biomarkers for pancreatic cancer-associated new-onset diabetes to pancreatic cancer screening. Pathol Res Pract 214: 1923-1928, 2018.
27. Cheng WP, Lo HM, Wang BW, Chua SK, Lu MJ and Shyu KG: Atorvastatin alleviates cardiomyocyte apoptosis by suppressing TRB3 induced by acute myocardial infarction and hypoxia. J Formos Med Assoc 116: 388-397, 2017.
28. Dobens LL, Nauman C, Fischer Z and Yao X: Control of cell growth and proliferation by the tribbles pseudokinase: Lessons from drosophila. Cancers (Basel) 13: 883, 2021.
29. Lee SK, Park CY, Kim J, Kim D, Choe H, Kim JH, Hong JP, Lee YJ, Heo Y, Park HS and Jang YJ: TRIB3 is highly expressed in the adipose tissue of obese patients and is associated with insulin resistance. J Clin Endocrinol Metab 107: e1057-e1073, 2022.
30. Ord T and Ord T: Mammalian pseudokinase TRIB3 in normal physiology and disease: Charting the progress in old and new avenues. Curr Protein Pept Sci 18: 819-842, 2017.
31. Bowers AJ, Scully S and Boylan JF: SKIP3, a novel Drosophila tribbles ortholog, is overexpressed in human tumors and is regulated by hypoxia. Oncogene 22: 2823-2835, 2003.
32. Loo LW, Tiirikainen M, Cheng I, Lum-Jones A, Seifried A, Church JM, Gryfe R, Weisenberger DJ, Lindor NM, Gallinger S, *et al*: Integrated analysis of genome-wide copy number alterations and gene expression in microsatellite stable, CpG island methylator phenotype-negative colon cancer. Genes Chromosomes Cancer 52: 450-466, 2013.
33. Yang K, Li B, Xu X, Yu Z, Lyu X, Ren K, Liu X, Chen S and Li H: TRIB3 overexpression predicts malignant progression and poor prognosis in human solid tumors: Bioinformatics validation and clinical significance. Expert Rev Mol Diagn 1-12 2024 (Epub ahead of print).
34. Zhou H, Luo Y, Chen JH, Hu J, Luo YZ, Wang W, Zeng Y and Xiao L: Knockdown of TRB3 induces apoptosis in human lung adenocarcinoma cells through regulation of Notch 1 expression. Mol Med Rep 8: 47-52, 2013.
35. Hua F, Shang S, Yang YW, Zhang HZ, Xu TL, Yu JJ, Zhou DD, Cui B, Li K, Lv XX, *et al*: TRIB3 Interacts With β-Catenin and TCF4 to increase stem cell features of colorectal cancer stem cells and tumorigenesis. Gastroenterology 156: 708-721.e15, 2019.
36. Shang S, Yang YW, Chen F, Yu L, Shen SH, Li K, Cui B, Lv XX, Zhang C, Yang C, *et al*: TRIB3 reduces CD8(+) T cell infiltration and induces immune evasion by repressing the STAT1-CXCL10 axis in colorectal cancer. Sci Transl Med 14: eabf0992, 2022.
37. Zhang W, Liu J, Tian L, Liu Q, Fu Y and Garvey WT: TRIB3 mediates glucose-induced insulin resistance via a mechanism that requires the hexosamine biosynthetic pathway. Diabetes 62: 4192-4200, 2013.

38. Pan D, Xu L and Guo M: The role of protein kinase C in diabetic microvascular complications. Front Endocrinol (Lausanne) 13: 973058, 2022.
39. Schultze SM, Hemmings BA, Niessen M and Tschopp O: PI3K/AKT, MAPK and AMPK signalling: protein kinases in glucose homeostasis. Expert Rev Mol Med 14: e1, 2012.